Communications in Physics, Vol. 32, No. 3 (2022), pp. 253-263
DOI: https://doi.org/10.15625/0868-3166/16737

# LIQUID-GATED FIELD-EFFECT-TRANSISTOR BASED ON CHEMICALLY REDUCED GRAPHENE OXIDE FOR SENSING NEUROTRANSMITTER ACETYLTHIOCHOLINE

NGUYEN THI THANH NGAN[1,†], NGUYEN DANH THANH[1], NGUYEN THI LAN[2], DUONG THANH TUNG[2], CAO THI THANH[3], NGUYEN VAN CHUC[3] AND VU THI THU[1]

[1]*University of Science and Technology of Hanoi, Vietnam Academy of Science and Technology, 18 Hoang Quoc Viet, Cau Giay, Hanoi, Vietnam*

[2]*Advanced Institute for Science and Technology, Hanoi University of Science and Technology, No.1 Dai Co Viet Road, Hai Ba Trung District, Hanoi, Vietnam*

[3]*Institute of Materials Science, Vietnam Academy of Science and Technology, 18 Hoang Quoc Viet, Cau Giay, Hanoi, Vietnam*

*E-mail:* [†]nguyen-thi-thanh.ngan@usth.edu.vn

*Received 16 November 2021*; *Accepted for publication 20 January 2022*; *Published 30 May 2022*

**Abstract.** *In this work, an enzymatic liquid-gated field-effect-transistor sensor based on chemically reduced graphene oxide film was developed for determination of acetylthiocholine in aqueous conditions. The device was designed with interdigitated electrode configuration and then manufactured by combining lithography and chemical vapor deposition techniques in clean room. Graphene oxide material (prepared by Hummer method) was chemically reduced using a strong reducing agent hydrazine, and then drop-casted onto the channel region. The X-Ray diffraction patterns and Raman spectra have clearly indicated an effective reduction of graphene oxide. Consequently, the transfer curve of as-prepared reduced graphene oxide based transistor exhibits ambipolar characteristics with a V-shape. Acetylcholinesterase was immobilized on top of reduced graphene oxide film with the aid of glutaraldehyde trapping agent. It was found that the release of proton from enzymatic hydrolysis of acetylthiocholine has caused significant variation in charge concentration and mobility in the channel, thus generated a significant blue shift in position of Dirac point on ambipolar curve. The developed sensor exhibits good sensing performances with LOD of 250 $\mu M$ and sensitivity of 2.0 $\mu A.\ mM^{-1}.cm^{-1}$ in concentration range 0 – 0.8 mM.*

Keywords: acetylcholinesterase; FET; graphene oxide; hydrazine.

Classification numbers: 87.85.fk.

## I. INTRODUCTION

The use of graphene and its derivatives in electronic sensors has recently attracted increasing attention for their high conductivity and many other chemical, optical and electrical behaviors [1–6]. However, the massive production of graphene is really limited since it requires expensive instruments and strict conditions. Thus, reduced graphene oxide (rGO) which can be easily synthesized and manipulated in aqueous conditions can be considered to be one of the best candidates to replace graphene [7–11]. To achieve reduced form of graphene oxide, it is essential to control the reduction process in which almost intrinsic oxygen-containing groups (carboxylic, hydroxyl, epoxy) in graphene oxide (GO) are eliminated [12, 13]. The restored sp2 carbon atoms in reduced graphene oxide makes this material similar to graphene in term of electrical behaviors as well as other physical properties. In the same time, the residual functional groups remained after reduction process (if any) might even facilitate the immobilization of targeted molecules (i.e, biomolecules) for further applications in biosensors [14–17].

The field-effect transistors (FETs) have recently been utilized in bio-sensing applications due to their high sensitivity, miniaturization, and real-time capability [17–20]. In principle, field effect transistor is an electronic device in which the variation of applied electric field leads to changing the current across the semiconductor channel between two electrodes (source and drain). In FET biosensors, a bio-recognition element is generally immobilized onto the surface of device channel so that the interaction between targeted molecules (substrate, antigen...) and relevant recognition element (enzyme, antibody) can be transduced into measurable signals [21, 22]. In order to improve the sensitivity of FET sensors, the channel is usually functionalized with highly conductive materials. rGO with high charge mobility, tunable ambipolar field-effect characteristics and biocompatibility [23] is probably a very promising material for improving performances of FET biosensors [24–26].

In this work, we develop an enzymatic rGO-based liquid-gated field effect transistor for determination of neurotransmitter acetylthiocholine (ATCh). rGO was prepared from graphene oxide via chemical reduction using hydrazine as reducing agent. The quality of GO and rGO was examined by XRD and Raman techniques. rGO was then deposited onto the channel in order to enhance the conductivity and compatibility of FET device. Acetylcholinesterase (AChE), which is a bio-catalyst for hydrolysis of acetylthiocholine, was then immobilized on the rGO-modified FET channel via cross-linking method using glutaraldehyde. The concentration of acetylthiocholine will be later recorded via the shift of Dirac point on transfer curve of as-developed rGO-based FET device.

## II. EXPERIMENT

### II.1. Chemical preparation of rGO

To have the rGO, firstly, the GO was prepared by the well-known modified Hummer's method as described previously [27]. In this method, the graphene layers from the natural graphite flakes are intercalated by adding suitable chemical species ($H_2SO_4$ and $NaNO_3$). The oxidation processes happen when KMnO4 was added into these intercalated graphene layers and forming pristine graphene oxide (PGO). The reaction between PGO and water converts the PGO to GO.

In contrast to the GO fabrication process, which required a strong oxidant to be able to oxidize the graphene layer to GO, the rGO synthesis process requires a reducing agent to be able

to remove GO functional groups. In this work, the prepared GO was reduced by using hydrazine hydrate solution. In detail, 3g synthesized GO was dispersed in a ratio of 1/4 of DI water/ethanol solution and sonicated for 2h. Hydrazine hydrate was then added at a weight ratio of 1:3 comparing to GO. The final solution was kept at 7 mg/ml concentration and stirred at 80˚C for 24h. The obtained black powder, rGO, was filtered and dried in a vacuum oven at 50˚C for 24h. Fig. 1 shows the whole synthesized process of rGO. The quality of rGO product was characterized by Raman spectroscopy and X-ray diffraction pattern.

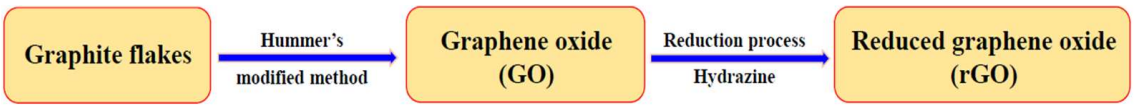


**Fig. 1.** Flowchat of reduced graphene oxide (rGO) preparation process.

### II.2. Fabrication of rGO based FET devices

The FET configuration using in this work includes interdigitated electrodes served as source and drain electrodes associated with a platinum top gate electrode. To construct the source (S) and drain (D) interdigitated electrodes, photolithography and thermal evaporation techniques were utilized. In brief, the silicon substrate with 300 nm oxide layer was treated with a standard cleaning procedure and then covered by an AZ 5214E photoresist layer. After removing the solvent by soft-bake, this wafer is exposed with a pre-designed mask for 2 seconds and then following by 120˚C for 2 minutes baking. The pattern which is appeared after development was deposited by co-evaporator system with gold material. Final structures were obtained by lift-off in acetone solution.

The synthesized rGO (0.1 mg/ml) was drop-casted onto the FET electrodes and then thermally annealed at 60oC for 10h. The covering rGO layer must be sufficiently large to cover all interdigitated electrodes and except the source and drain measurement pads.

### II.3. Acetylcholinesterase FET sensor

Enzyme acetylcholinesterase (10 U/µl) and acetylthiocholine (50 mM) were prepared in PBS solution and stored in deep frigde at -20˚C. 5 $\mu$l enzyme acetylcholinesterase (AChE) was immobilized onto rGO modified FET channel with using GA (glutaraldehyde) as cross-linking agent at 4˚C for 120 minutes. The electrical properties of this device were characterized by using a 4-probe station "Keithley 4200-SCS".

## III. RESULTS AND DISCUSSIONS

### III.1. rGO formation

X-ray diffraction (XRD) patterns of GO and rGO were recorded with using Cu $K_\alpha$ radiation ($\lambda = 0.154184$ nm) (Fig. 2). GO exhibited a peak at $2\lambda = 10.9^\circ$ ($d = 0.811$ nm) corresponding to the (002) reflection plane and interlayer distance of 0.811 nm, and a very small peak at $2\lambda = 22.4^\circ$ ($d = 0.397$ nm) remained from raw graphite powder. It seems that the reduction in Hummer method is not really complete even with using such strong oxidizing agents due to stacking effect in graphite material. The increase in interplanar distance is probably resulted from the intercalation

of water molecules and the formation of oxygenated functional groups at basal planes and edges of graphite flakes during oxidation process. Meanwhile, rGO only shows a broad peak located at $2\lambda = 23.9^{\circ}$ ($d = 0.372$ nm) relevant to (002) reflection plane of graphite structure (JCPDS 75-2078), indicating a successful reduction of GO to form rGO [28,29]. The tiny peak in XRD pattern of rGO at $2\lambda = 44^{\circ}$ is attributed to the turbostratic band of disordered carbon materials [30, 31].

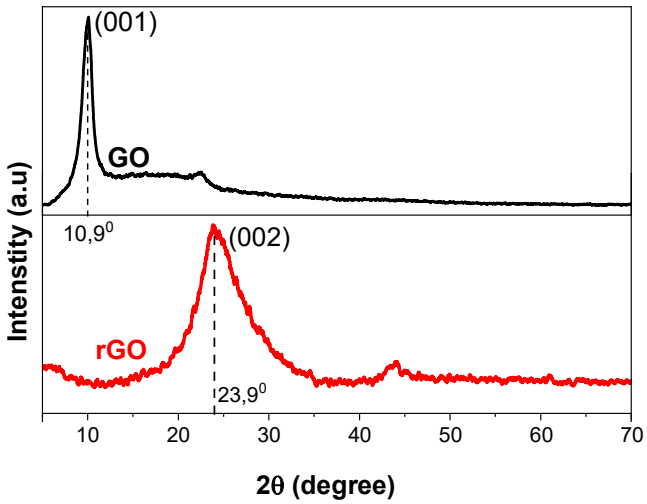


**Fig. 2.** XRD pattern of GO and rGO.

The Raman spectra of GO and rGO (Fig. 3) show the consistency with the XRD results. Both GO and rGO have two most intensive peaks, corresponding to the so-called D-band and G-band. The G-band represents the symmetry and crystallinity of the material, while D-band reflects the defects and disorders. In the case of GO, these two peaks were observed at 1370 $cm^{-1}$ for the D-band and 1590 $cm^{-1}$ for the G-band. Whereas, these bands in the rGO sample are slightly shifted to 1320 $cm^{-1}$ and 1600 $cm^{-1}$, respectively. This effect indicates a higher disorder level of the graphene layers and increasing the defect numbers after the reduction of GO. Besides, the intensity ratio between D-band and G-band in rGO (ID/IG = 1.21) is slightly higher than that in GO (ID/IG = 0.79), suggesting the presence of a more isolated graphene domain and the removal of a large number of oxygen-containing functional groups in rGO [32, 33]. In fact, the ID/IG ratio is not a reliable parameter to evaluate the disorder of material because for the small crystallite size ($\sim$ 2 nm) this ratio increases with order [34]. Another parameter which has been suggested to evaluate the disorder is the width of D and G peaks [35]. The fitting results of these peaks one more time confirmed the region of the increasing disorder. These results are comparable with the previous studies [36, 37].

### III.2. rGO based FET devices

The interdigitated geometry is widely used in modern electronic devices since it has a wide contact area between the electrodes within a limited area, and thus would give higher efficiency. The interdigitated electrodes design used in this work has the same configuration as described in

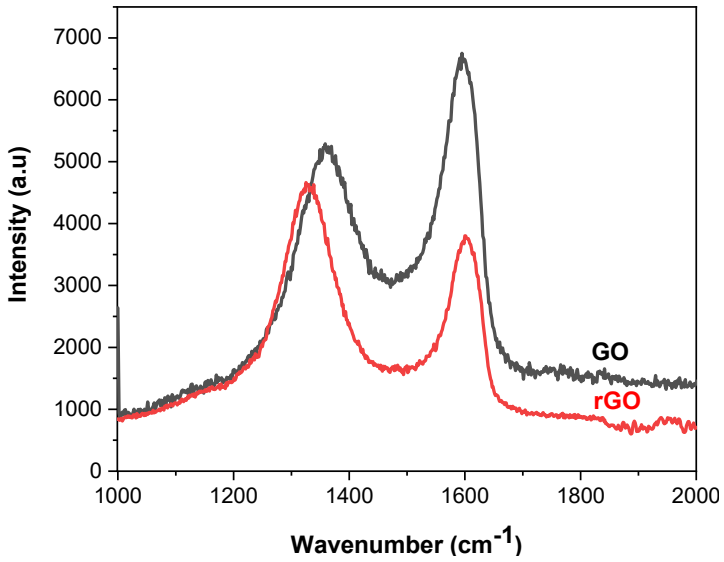


**Fig. 3.** (color online) Raman spectra of the synthesized GO and rGO.

our previous report [38]. The morphology of drain and source channels of interdigitated electrodes coated with and without rGO were examined by SEM. As we can see in Fig. 4, the rGO layer covered all the area of interdigitated electrodes. The inset image showed details of the rGO wrinkles. The source and drain electrodes include ten lines for each one in which each line has a width of 60 $\mu$m and a length of 2500 $\mu$m [38, 39]. The distance between them was 50 μm. The decrease of line width and their space may enhance the obtained signal, but the limitation of the mask fabrication method does not allow the higher solution.

The rGO functionalized FET was then evaluated electric properties by transfer characteristic. The transfer curve represents an ambipolar property of FET that is capable of both electron and hole transport [40, 41]. The transition between two conducting regimes is identified through a value of voltage called Dirac point which is the minimum value in the relationship between the gate voltage and drain-source current. The drain-source current (or channel current) is given by following equation [42]:

$$I_D S = \frac{W}{2L} C_d l \mu (V_{GS} - V_{th})^2 \quad (1)$$

where $W$, $L$ are the width and length of FET channel, respectively, Vth threshold voltage, $V_{GS}$ gate-source voltage, Cdl capacitance of electrical double layer, and $\mu$ is the charge carrier mobility.

The drain-source current (IDS) was measured while the gate voltage (VGS) was swept from 1.0 to 4.5 V. As seen in Fig. 5, there was a Dirac point, which is defined as the VGS value at which the minimum IDS, at 2.4 V. This result indicates that the conductivity of rGO was altered by the field effect and the type of charge carrier was changed.

### III.3. Sensing performance

Acetylcholinesterase sensors can be employed to determine the level of acetylcholine – an important neurotransmitter - in human body fluids, or detect some neurotoxins such as sarin,

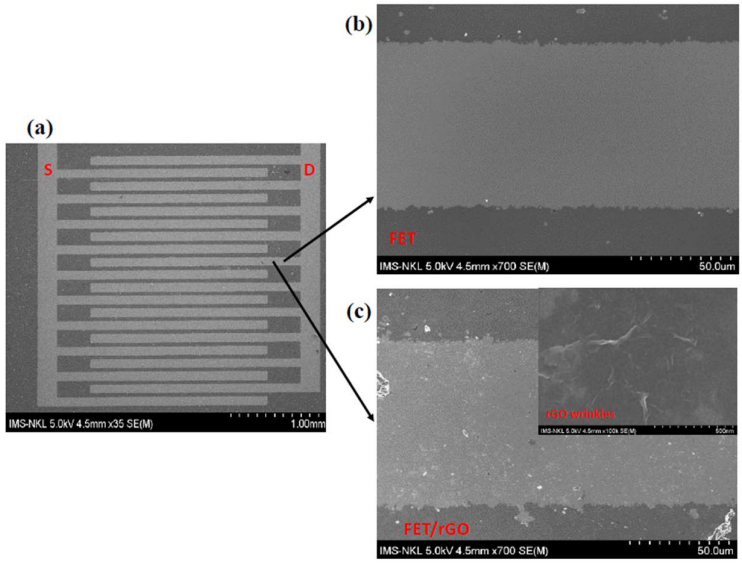


**Fig. 4.** SEM images of (a) interdigitated electrodes of FET device, (b) one line of FET channel without the coated rGO layer and (c) one line of FET channel with rGO-modified layer. The inset shows the rGO winkles of detail.

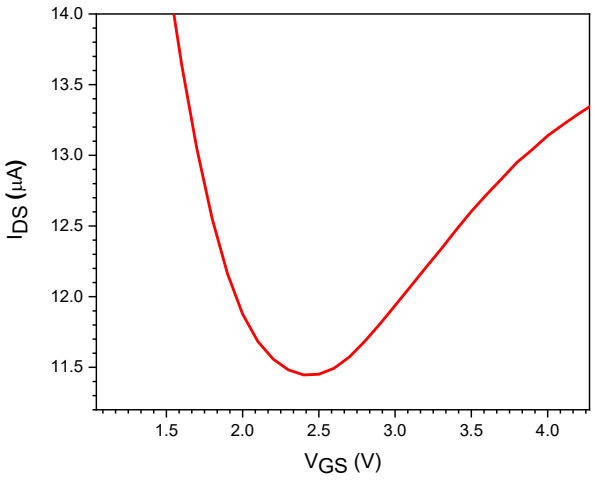


**Fig. 5.** Transfer characteristic of bare FET/rGO. The Dirac point was located at $V_{GS} = 2.4$ V.

organophosphates, carbamates. Herein, acetylcholinesterase was fixed onto rGO modified FET channel for further application in determination of acetylthiocholine level. The immobilization of enzyme was assisted by glutaraldehyde cross-linking agent which provide a net to trap enzyme on the channel surface. In the same time, the residual oxygenated functional groups such as –OH, –COOH in rGO after reduction process might also help to improve the adhesion of enzyme molecules onto the channel of FET device.

The hydrolysis of acetylthiocholine (ATCh) with the aid of acetylcholinesterase (AchE) [43] can be depicted as follows:

$$\mathrm{ATCh} + \mathrm{H_2O} \xrightarrow{\mathrm{AChE}} \mathrm{Thichocholine} + \mathrm{CH_3COOH}. \quad (2)$$

This enzymatic reaction will release the H+ ions (from the acid acetic $CH_3COOH$). These produced ions then can be used as an indicator to determine the concentration of ATCh molecules. The interaction between protons releasing from the enzymatic reaction and rGO material might lead to the change in charge concentration and mobility at the FET channel [44]. Consequently, the Dirac point which is ambipolar characteristic of carbonaceous material (seen in Fig. 4) might be shifted.

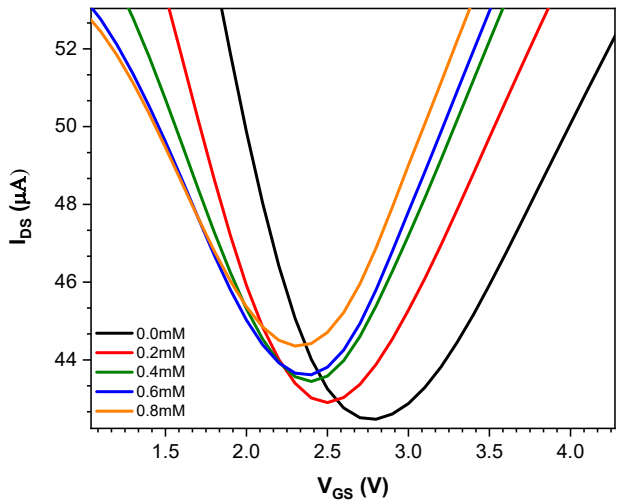


**Fig. 6.** (color online) Transfer characteristic of sensor with different ATCh concentrations.

Figure 6 shows the drain-source current (IDS) plotted as a function of gate voltage (VGS) at different concentrations of ATCh ranging from 0.0 mM to 0.8 mM. In this measurement, the VDS was kept at 0.5 V and the gate voltage VGS was scanned from 1.0 to 4.5 V. When ATCh was not added yet, the minimum of the current (or Dirac point) is observed at 2.8 V. This slight shift of Dirac point by 0.4 V (compared with rGO modified channel) is directly related to the presence of enzyme molecules which are not highly conductive. When ATCh is introduced, the Dirac point was slightly shifted toward lower potentials (Fig. 7a) whereas the current response was increased (Fig. 7b). The linear relation of conductance and ATCh concentration (Fig. 7a) indicates that the higher ATCh concentration corresponding with the higher number of $H^+$ ions release and higher mobile charges on the FET/rGO channel. This result is in accordance with previous reports [14,43]. The limit of detection (LOD) value determines by five calibration points from the 0 mM to 0.8 mM concentration of ATCh. The obtained value is 250 $\mu$M, which seems not to be comparable to the case of using graphene in the channel [38]. This result might be due to the order of the reduction process, in which some residual oxygen functional groups lead to the lower conductivity of rGO. The sensitivity was estimated to be 2.0 $\mu\mathrm{A.mM^{-1}.cm^{-1}}$.

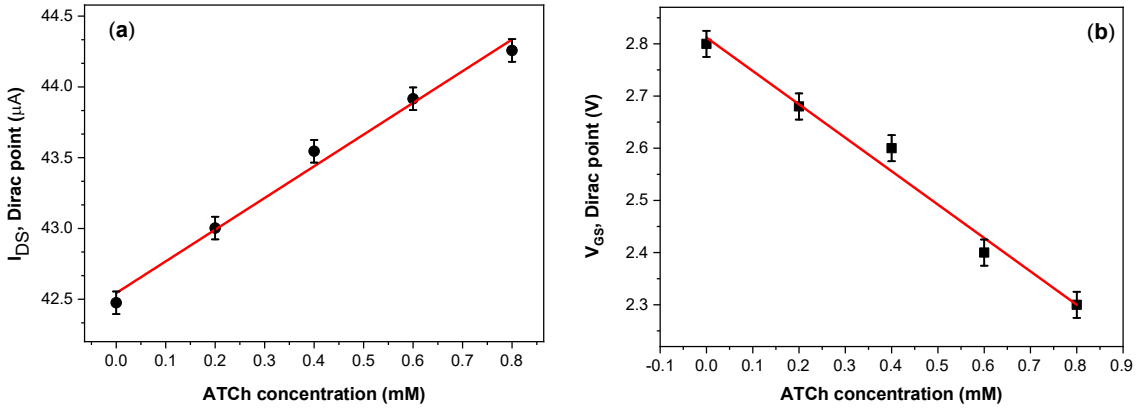


**Fig. 7.** Dirac point current (a) and voltage (b) as a function of ATCh concentration.

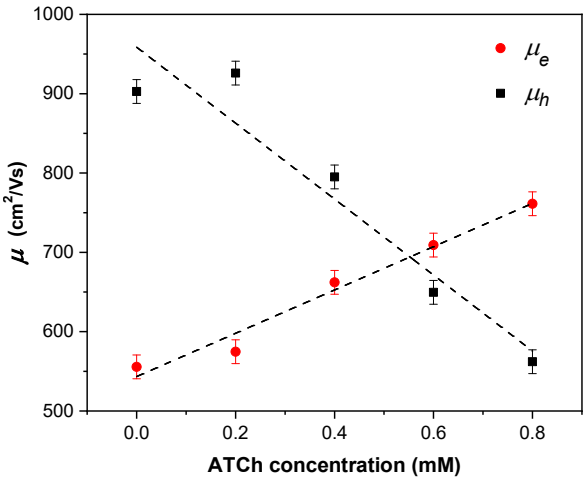


**Fig. 8.** Electron and hole mobility with different ATCh concentrations. (Obtained from the fits of transfer curve in Fig. 5).

The electron and hole mobility derived from fits of the transfer curves and their dependence on the ATCh concentration through the following formula [45]:

$$\mu = m_{\text{linear}} \frac{L}{W V_{DS} C_i},$$

where $m_{\text{linear}}$ is the slope of the transfer curves linear fit, L and W are the length and width of the channel, respectively. $V_{DS}$ is the applied source-drain voltage and $C_i$ is the top gate capacitance ($C_i = 1.2\ \mu$F/cm$^2$) [38, 45]. It can be seen in Fig. 8, the highest the hole mobility reaches a value of $\sim$950 cm$^2$/Vs while this value of electron mobility is only $\sim$750 cm$^2$/Vs. These values are much higher than that obtained on rGO channel without enzyme (hole and electron mobility are only 270 cm$^2$/Vs and 78 cm$^2$/Vs, respectively).

The mobility of the hole and electron also show opposite trends. The hole mobility decreases as increase of ATCh concentration and vice versa with electron mobility. At the lower ATCh concentration, the holes are majority charge carriers, while electrons dominate at higher ATCh concentrations. There is one point between 0.5 to 0.6 mM of ATCh concentration which could be called "iso-mobility point". At this point, the mobility of electron and hole are about equal, similar to the isoelectric point [45].

## IV. CONCLUSIONS

In this work, we have fabricated FET device with the channel modified by the rGO material for further application in the detection of ATCh molecules. We measured the Dirac voltage shift as a function of ATCh concentration and found that the concentrations of H+ ions released during the hydrolysis of ATCh lead to an increase in charge numbers on the FET/rGO channel. The conductance of the device, as a consequence, increases with the increase of ATCh concentration whereas the Dirac point voltages diminish. This work contributes one puzzle piece to the modification of FET channel by using carbonaceous materials. Although the LOD of rGO-based FET is not comparable to graphene-based FET, the simple and massive preparation makes it becomes a promising sensing platform. It is essential to control better reduction process to obtain higher quality of rGO material in near future.

## ACKNOWLEDGEMENT

This research is supported by Vietnam Academy of Science and Technology under the grant number QTFR01.02/19-20 and NAFOSTED 103.02-2018.360. We also would like to express our great thanks to our colleagues at Nano and Energy Center (NEC), Hanoi University of Science for their kindly support in FET fabrication and our colleagues at Advanced Institute for Science and Technology (AIST), Hanoi University of Science and Technology for providing graphene oxide material.

## REFERENCES

[1] P. Aspermair, V. Mishyn, J. Bintinger, H. Happy, K. Bagga, P. Subramanian, W. Knoll, R. Boukherroub and S. Szunerits, *Reduced graphene oxide–based field effect transistors for the detection of E7 protein of human papillomavirus in saliva*, *Anal. Bioanal. Chem.* **413** (2021) 779.

[2] X. Sui, H. Pu, A. Maity, J. Chang. B. Jin, G. Lu, Y. Wang, R. Ren, S. Mao and J. Chen, *Field effect transistor based on percolation network of reduced graphene oxide for real-time ppb-level detection of lead ions in water*, *ECS J. Solid State Sci. Technol.* **9** (2020) 115012.

[3] J. Sengupta and C. M. Hussain, *Graphene-based field-effect transistor biosensors for the rapid detection and analysis of viruses: A perspective in view of COVID-19*, *Carbon Trends* **2** (2021) 100011 100019.

[4] Q. He, S. Wu, Z. Yin and H. Zhang, *Microvesicle detection by a reduced graphene oxide field-effect transistor biosensor based on a membrane biotinylation strategy*, *Chem. Sci.* **3** (2012) 1764.

[5] M. Kurian, *Recent progress in the chemical reduction of graphene oxide by green reductants–A Mini review*, *Carbon Trends* **5** (2021) 100120.

[6] A. G. Olabi, M. A. Abdelkareen, T. Wilberforce and E. T. Sayed, *Application of graphene in energy storage device – A review*, *Renew. Sust. Energ. Rev.* **135** (2021) 110026.

[7] D. Wu, H. Zhang, D. Jin, D. W. Pang, M. M. Xiao, Z. L. Zhang and Z. Y. Zhang, *Microvesicle detection by a reduced graphene oxide field-effect transistor biosensor based on a membrane biotinylation strategy*, *Analyst* **144** (2019) 6055.

[8] T. Q. Trung, N. T. Tien, D. Kim, M. Jang, O. J. Yoon and N. –E. Lee, *A flexible reduced graphene oxide field-effect transistor for ultrasensitive strain sensing*, *Adv. Funct. Mater.* **24** (2013) 117.

[9] C. R. Rozman, A. Kotlowski and W. Knoll, *Electronic biosensing with functionalized rGO FETs*, *Biosensors* **6** (2016) 17.

[10] M. Hasegawa, Y. Hirayama, Y. Ohno, K. Maehashi and K. Matsumoto, *Characterization of reduced graphene oxide field-effect transistor and its application to biosensor*, *Jpn. J. Appl. Phys.* **53** (2014) 05FD05.

[11] N. Sharma, V. Sharma, Y. Jain, M. Kumari, R. Gupta, S. K. Sharma and K. Sachdev, *Synthesis and characterization of graphene oxide (GO) and reduced graphene oxide (rGO) for gas sensing application*, *Macromol. Symp.* **376** (2017) 1700006.

[12] Z. Shahryari, M. Yeganeh, K. Gheisari and B. Ramezanzadeh, *A brief review of the graphene oxide-based polymer nanocomposite coatings: preparation, characterization, and properties*, *J. Coat. Technol. Res.* **18** (2021) 945.

[13] V. Agarwal and P. B. Zetterlund, *Strategies for reduction of graphene oxide – A comprehensive review*, *Chem. Eng. J.* **405** (2021) 127018.

[14] T. Quast, F. Mariani, E. Scavetta, W. Schuhmann and C. Andronescu, *Reduced-graphene-oxide-based needle-type field-effect transistor for dopamine sensing*, *ChemElectroChem* **7** (2020) 1922.

[15] M. Sun, C. Zhang. D. Chen, J. Wang, Y. Ji, N. Liang, H. Gao, S. Cheng and H. Liu, *Ultrasensitive and stable all graphene field-effect transistor-basedHg2+ sensor constructed by using different covalently bonded RGO films assembled by different conjugate linking molecules*, *SmartMat.* **2** (2021) 213.

[16] H. Yu, W. Guo, X. Lu, H. Xu, Q. Yang, J. Tan and W. Zhang, *Reduced graphene oxide nanocomposite based electrochemical biosensors for monitoring foodborne pathogenic bacteria: A review*, *Food Control* **127** (2021) 108117.

[17] K. Nakama, M. Sedki, A. Mulchandani, *Label-free chemiresistor biosensor based on reduced graphene oxide and M13 bacteriophage for detection of coliforms*, *Anal. Chim. Acta* **1150** (2021) 338232.

[18] L. Chao, Y. Liang, X. Hu, H. Shi, T. Xia, H. Zhang and H. Xia, *Recent advances in field effect transistor biosensor technology for cancer detection: a mini review*, *J. Phys. D: Appl. Phys.* **55** (2022) 153001.

[19] Y. C. Syu, W. E. Hsu, C. T. Lin, *Review—field-effect transistor biosensing: devices and clinical applications*, *ECS J. Solid State Sci. Technol.* **7** (2018) Q3196.

[20] T. Wadhere, D. Kakkar, G. Wadhwa, B. Raj, *Recent advances and progress in development of the field effect transistor biosensor: A Review*, *J. Electron. Mater.* **48** (2019) 7635.

[21] L. Syedmoradi, A. Ahmadi, M. L. Norton and K. Omidfar, *A review on nanomaterial-based field effect transistor technology for biomarker detection*, *Microchimica Acta* **186** (2019) 739.

[22] I. Novodchuk, M. Bajcsy and M. Yavuz, *Graphene-based field effect transistor biosensors for breast cancer detection: A review on biosensing strategies*, *Carbon* **172** (2021) 431.

[23] A. D. Rashid, A. R. Ruslinda, M. F. Fatin, U. Hashim and M. K. Arshad, *Fabrication and characterization on reduced graphene oxide field effect transistor (RGOFET) based biosensor*, *AIP Conf. Proc.* **1733** (2015) 020076.

[24] X. Jin, H. Zhang, Y. T. Li, M. M. Xiao, Z. L. Zhang, D. W. Pang, G. Wong, Z. Y. Zhang and G. J. Zhang, *A field effect transistor modified with reduced graphene oxide for immunodetection of Ebola virus Xin*, *Microchimica Acta* **186** (2019) 223.

[25] M. S. Chae, Y. K. Yoo, J. Kim. T. G. Kim. K. S. Hwang, *Graphene-based enzyme-modified field-effect transistor biosensor for monitoring drug effects in Alzheimer's disease treatment*, *Sens. Actuators B Chem.* **272** (2018) 448.

[26] P. Bhattacharyya, *Fabrication strategies and measurement techniques for performance improvement of graphene/graphene derivative based FET gas sensor devices: A review*, *IEEE Sensors J.* **21** (2021) 10231.

[27] N. T. Lan, D. T. Chi, N. X. Dinh, N. D. Hung, H. Lan, P. A. Tuan, L. H. Thang, N. N. Trung, N. Q. Hoa, T. Q. Huy. N. V. Quy, T. T. Duong, V. N. Phan and A. T. Le, *Photochemical decoration of silver nanoparticles on graphene oxide nanosheets and their optical characterization*, *J. Alloys Compd.* **615** (2014) 843.

[28] H. S. Maharana, P. K. Rai and A. Basu, *Surface-mechanical and electrical properties of pulse electrodeposited Cu–graphene oxide composite coating for electrical contacts*, *J. Mater Sci.* **52** (2017) 1089.

[29] A. Shalaby, D. Nihtianova, P. Markov, A. D. Staneva, R. S. Iordanova and Y. B. Dimitriev, *Structural analysis of reduced graphene oxide by transmission electron microscopy*, *Bulg. Chem. Commun.* **47** (2015) 291.

[30] M. R. Martínez, M. A. Álvarez, M. V. L. Ramón, G. C. Quesada, J. R. Utrilla and M. S. Polo, *Hydrothermal synthesis of rGO-TiO_2 composites as high-performance UV photocatalysts for ethylparaben degradation*, *Catalysts* **10** (2020) 520.

[31] K. Dave, K. H. Park and M. Dhayal, *Two-step process for programmable removal of oxygen functionality of graphene oxide: functional, structural and electrical characteristics*, *RSC Adv.* **5** (2015) 95657.

[32] H. Su, C. Zhang, X. Li, L. Wu and Y. Chen, *Aggregation prevention: reduction of graphene oxide in mixed medium of alkylphenol polyoxyethylene (7) ether and 2-methoxyethanol*, *RSC Adv.* **8** (2018) 39140.

[33] D. Konios, M. M. Stylianakis, E, Stratakis and E. Kymakis, Dispersion behaviour of graphene oxide and reduced graphene oxide, *J. Colloid Interface Sci.* **430** (2014) 108.

[34] A. C. Ferrari, *Raman spectroscopy of graphene and graphite: Disorder, electron–phonon coupling, doping and nonadiabatic effects*, *Solid State Commun.* **143** (2007) 47.

[35] V. Scardaci and G. Compagnini, *Raman spectroscopy investigation of graphene oxide reduction by laser scribing*, *C* **7** (2021) 48.

[36] M. Srivastava, A. K. Das, P. Khanra, M. E. Uddin, N. H. Kim and J. H. Lee, *Characterizations of in situ grown ceria nanoparticles on reduced graphene oxide as a catalyst for the electrooxidation of hydrazine*, *J. Mater. Chem. A* **1** (2013) 9792.

[37] J. Ding, S. Zhu, T. Zhu, W. Sun, Q. Li, G. Wei and Z. Su, *Hydrothermal synthesis of zinc oxide-reduced graphene oxide nanocomposites for an electrochemical hydrazine sensor*, *RSC Adv.* **5** (2015) 22935.

[38] C. T. Thanh, N. H. Binh, N. V. Tu, V. T. Thu, M. Bayle, M. Pailler, J. L. Sauvajol, P. B. Thang, T. D. Lam, P. N. Minh and N. V. Chuc, *An interdigitated ISFET-type sensor based on LPCVD grown graphenefor ultrasensitive detection of carbaryl*, *Sens. Actuators B Chem.* **260** (2018) 78.

[39] T. T. Cao, V. C. Nguyen, H. B. Nguyen, H. T. Bui, T. T. Vu, N. H. Phan, B. T. Phan, l. Hoang. M. Bayle, M. Paillet, J. L. Sauvajol, N. M. Phan and D. L. Tran, *Fabrication of few-layer graphene film based field effect transistor and its application for trace-detection of herbicide atrazine*, *Adv. Nat. Sci.: Nanosci. Nanotechnol.* **7** (2016) 035007.

[40] M. S. Kang and C. D. Frisbie, *A pedagogical perspective on ambipolar FETs*, *ChemPhysChem* **14** (2013) 1547.

[41] C. Y. Lin, R. K. Ulaganathan, R. Sankar and F. C. Chou, *Ambipolar field-effect transistors by few-layer InSe with asymmetry contact metals*, *AIP Adv.* **7** (2017) 075314.

[42] Q. Zhang, F. Leonardi, A. Casalini, I. Temino and M. M. Torrent, *High performing solution-coated electrolyte-gated organic field-effect transistors for aqueous media operation*, *Sci. Rep.* **6** (2016) 39623.

[43] T. T. Vu, T. N. N. Dau, C. T. Ly, D. C. Pham, T. T. N. Nguyen and V. T. Pham, *Aqueous electrodeposition of (AuNPs/MWCNT–PEDOT) composite for high-affinity acetylcholinesterase electrochemical sensors*, J. Mater. Sci. **55** (2020) 9070.

[44] I. -Y. Sohn, D. -J. Kim, J. -H. Jung, O. J. Yoon, T. N. Thanh, T. T. Quang and N. -E. Lee, *pH sensing characteristics and biosensing application of solution-gated reduced graphene oxide field-effect transistors*, *Biosens. Bioelectron.* **45** (2013) 70.

[45] C. R. Rozman, M. Larisika, C. Nowak and W. Knoll, *Graphene-basedliquid-gated field effecttransistorfor-biosensing: Theory andexperiments*, *Biosens. Bioelectron.* **70** (2015) 21.